# Supplementary Information

Mesoporous Niobium-Doped Titanium Dioxide Films from the Assembly of Crystalline Nanoparticles: on the Relationship between Band Structure, Conductivity and Charge Storage Mechanism

Junpei Yue,[a] Christian Suchomski,[a] Pascal Voepel,[a] Ruediger Ellinghaus,[a] Marcus Rohnke,[a] Thomas Leichtweiss,[a] Matthias T. Elm[a,b] and Bernd M. Smarsly[a,*]
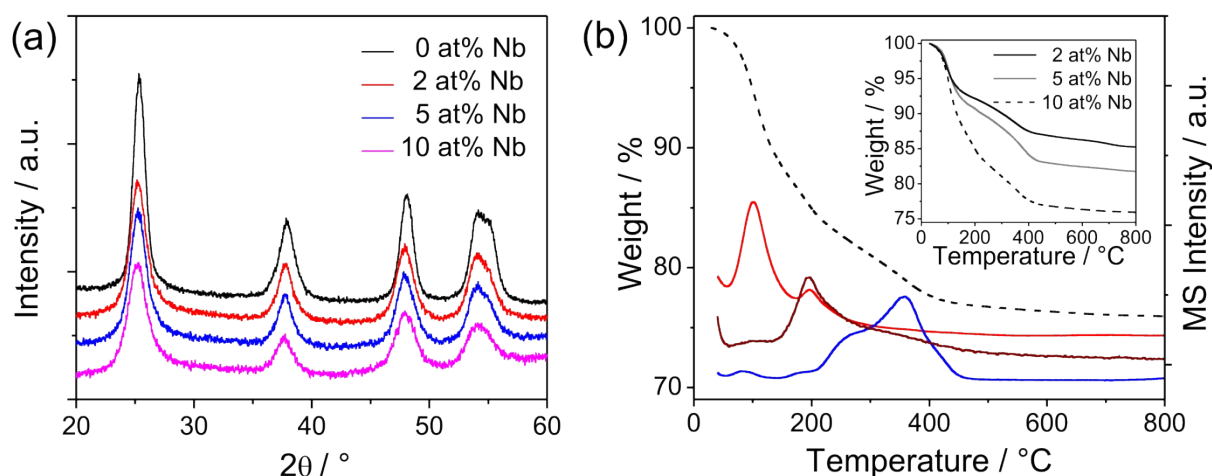
Figure S1. (a) XRD patterns of as-prepared TiO_2 and Nb-doped TiO_2 nanoparticles. The determined crystallite sizes are 4.7 nm (pure TiO_2), 4.9 nm (2 at% Nb), 4.9 nm (5 at% Nb) and 4.2 nm (10 at% Nb), respectively. (b) Combined thermogravimetric analysis/mass spectrometry (TGA−MS) data of as-prepared Nb-doped TiO_2 nanoparticles in synthetic air at 5 °C/min. A total mass loss of approx. 15%, 18% and 24% by 800 °C (inset) was observed for samples with 2 at% Nb, 5 at% Nb and 10 at% Nb, respectively. The MS analysis shows H_2O (*m/e* = 18, $I \times 0.5$) in red, HCl (*m/e* = 36, $I \times 10$) in brown and CO_2 (*m/e* = 44, $I \times 5$) in blue. As can be seen, adsorbed water molecules and solvent residues desorb in the temperature range between 60 and 200 °C, while the combustion of covalently bonded organic ligands (e.g., $C_6H_{13}O$) and the release of hydrochloric acid gas by thermal cleavage of Ti−Cl bonds were found to occur between 200 °C and 400 °C.
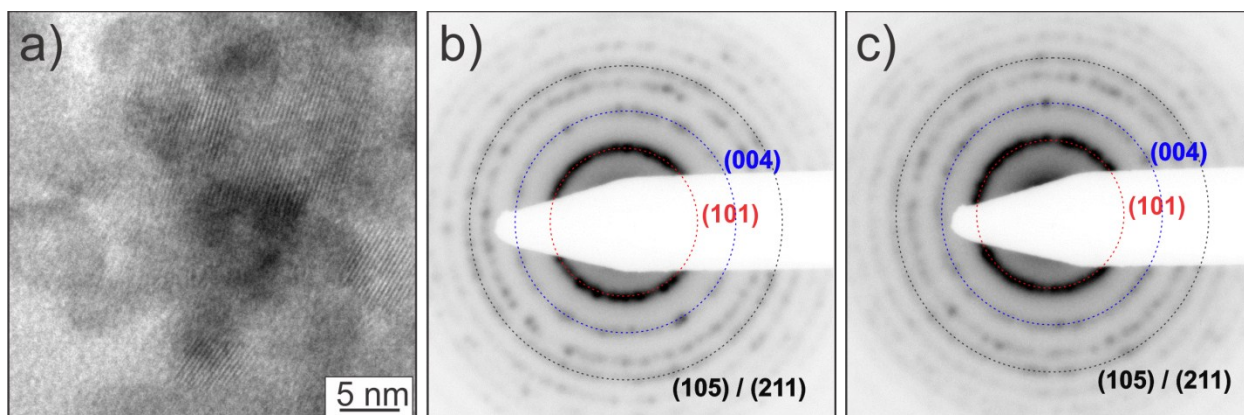
Figure S2. (a) Representative HRTEM image of as-prepared (2 at%) Nb-doped TiO$_2$ nanoparticle. (b, c) SAED patterns of doped TiO$_2$ nanoparticle for 2 at% Nb and 5 at% Nb.
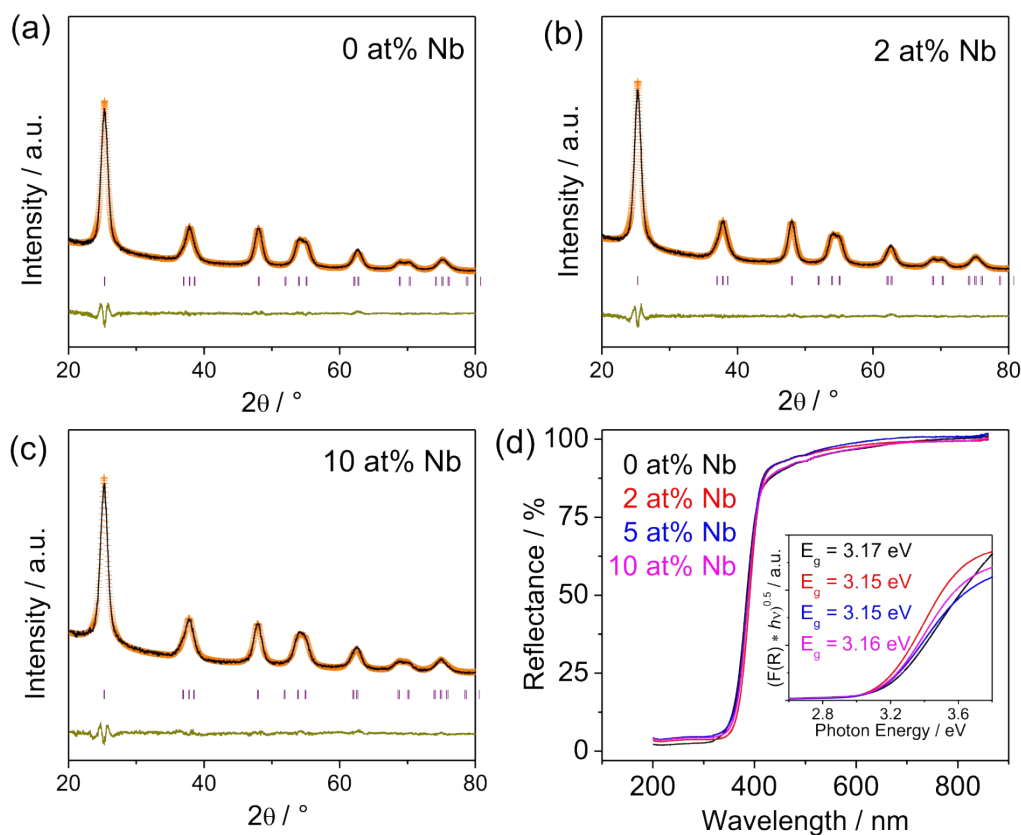

Figure S3. Rietveld refined XRD patterns of TiO$_2$ nanoparticles with different Nb doping level: (a) pure TiO$_2$; (b) 2 at% Nb and (c) 10 at% Nb. (d) UV-visible reflectance spectra of Nb-doped TiO$_2$ materials after heat treatment at 400 °C for 1 hour. The Tauc plot shown in the inset indicates indirect optical band gaps (E_g) at 3.17, 3.15, 3.15 and 3.16 eV (error margin ± 0.05 eV), respectively.

Table S1. Summary of refined structural parameters of doped TiO_2 nanoparticles after thermal treatment for 1 h at 400 °C. For purposes of comparison reference data are also given in Table **S2**.

Composition		TiO_2	2 at% Nb	5 at% Nb	10 at% Nb
Space group		$I4_1/amd$ (#141)			
Lattice parameters / (Å)	a, b	3.787	3.789	3.792	3.797
	c	9.508	9.511	9.520	9.528
Unit cell volume / Å³		136.59	136.62	136.94	137.53
Calc. density / g cm⁻³		4.159	4.156	4.128	4.311
Average grain size / nm		6.4	6.2	6.5	5.5
Average maximum microstrain / ×10⁻⁴		62	60	60	64
R_{wp} [Bragg contributions] / %		9.17	8.37	9.30	12.4
Goodness of fit, χ^2		1.75	1.55	2.08	3.21

**Table S2.** Structural parameters of nanocrystalline Nb-doped TiO_2 powder materials.

|	Unit cell volume / Å³			
	0 at% Nb	2 at% Nb	5 at% Nb	10 at% Nb
Own data	136.59	136.62	136.94	137.53
Chem. Mater. **2004**, *16*, 862-871.	136.2	136.4	136.6	137.4
J. Am. Chem. Soc. **2014**, *136*, 419−426.	136.5	137.1	137.9	138.8
Adv. Funct. Mater. **2014**, *24*, 5075–5085.	138.9		140.0	141.7
J. Mater. Chem. A **2015**, *3*, 22969–22974.	136.23	136.52	136.75	-
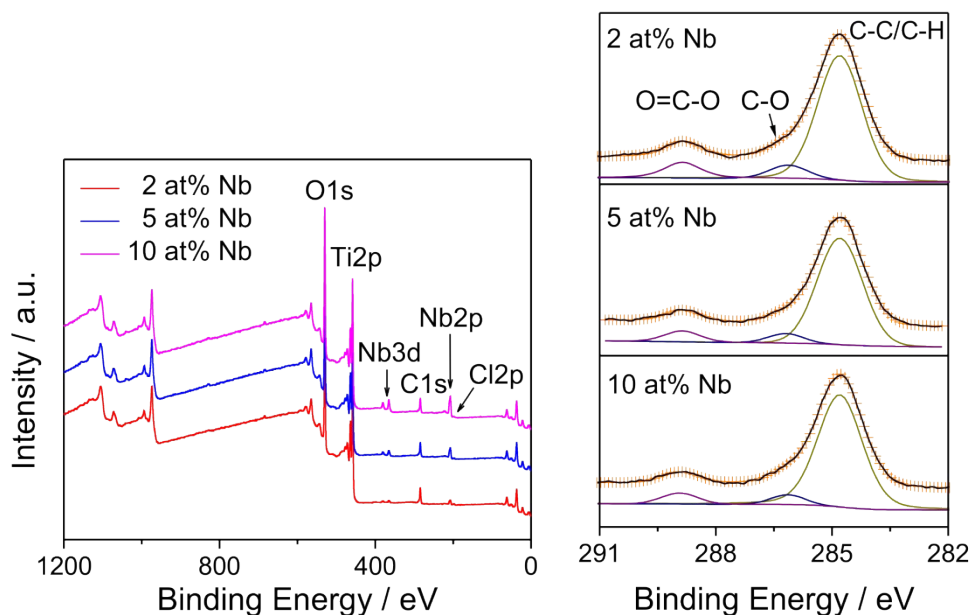
Figure S4. XPS survey spectra (left) and C 1s core level spectra (right) of as-prepared Nb-doped TiO_2 powder samples.

Table S3. XPS peak analysis data.

	Ti 2p$_{3/2}$ / eV			Nb 3d$_{5/2}$ / eV		
	2 at% Nb	5 at% Nb	10 at% Nb	2 at% Nb	5 at% Nb	10 at% Nb
Own data	458.8	458.7	Reduced Ti	207.4	207.4	Reduced Nb
Appl. Phys. Express **2008**,*1*, 111203.	-	458.7	yes	-	207.5	yes
Adv. Mater. **2009**, *21*, 2282–2287.	-	459.3	no	-	207.7	no
Adv. Funct. Mater. **2014**, *24*, 5075–5085.	458.5	458.3	yes	-	206.8	no
J. Mater. Chem. A **2015**, *3*, 22969–22974.	-	458.2	no	-	206.6	no
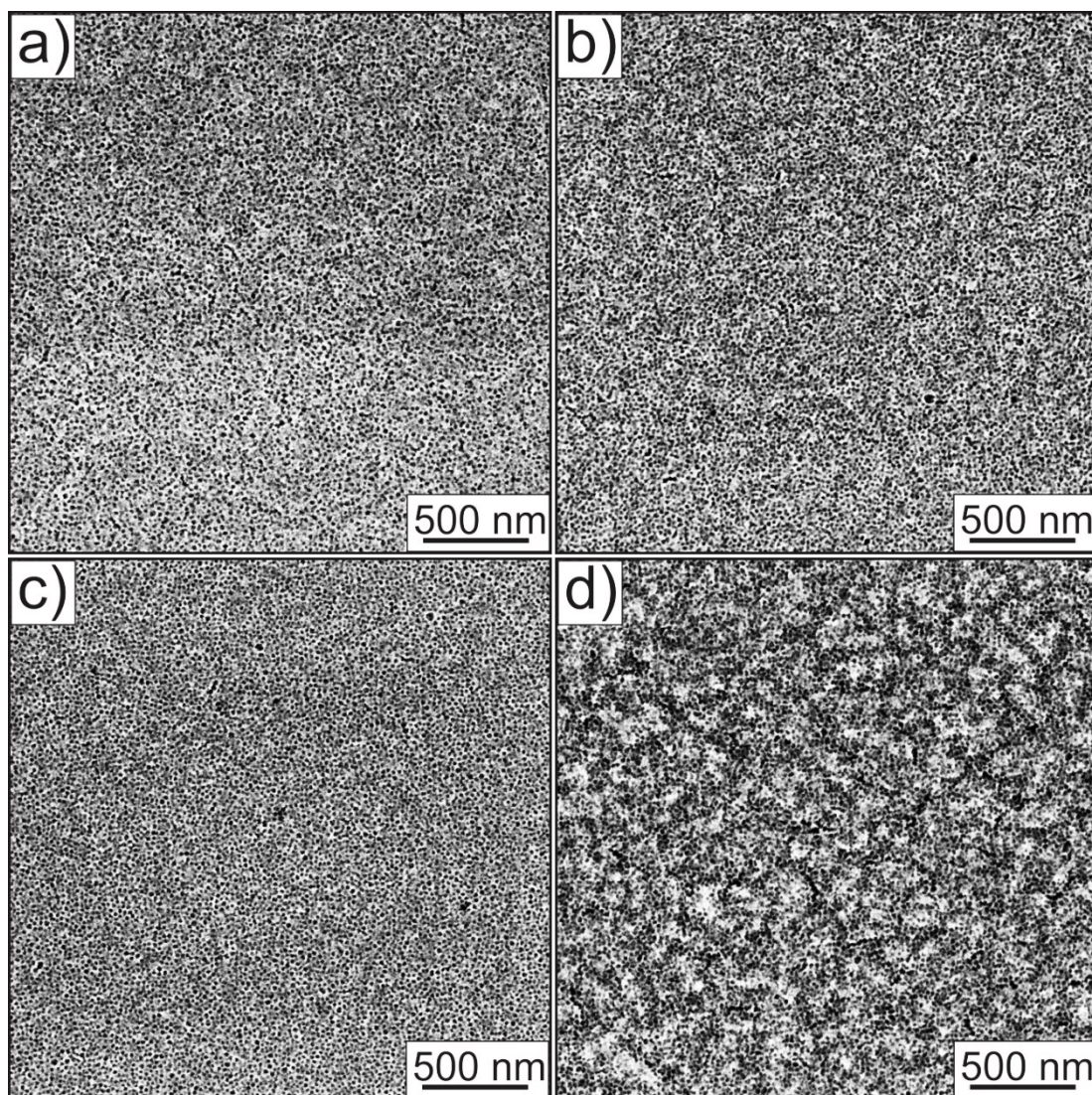
Figure S5. Top-view SEM images of mesoporous Nb-doped TiO$_2$ thin films. (a) pure TiO$_2$. (b) 2 at% Nb, (c) 5 at% Nb and (d) 10 at% Nb.
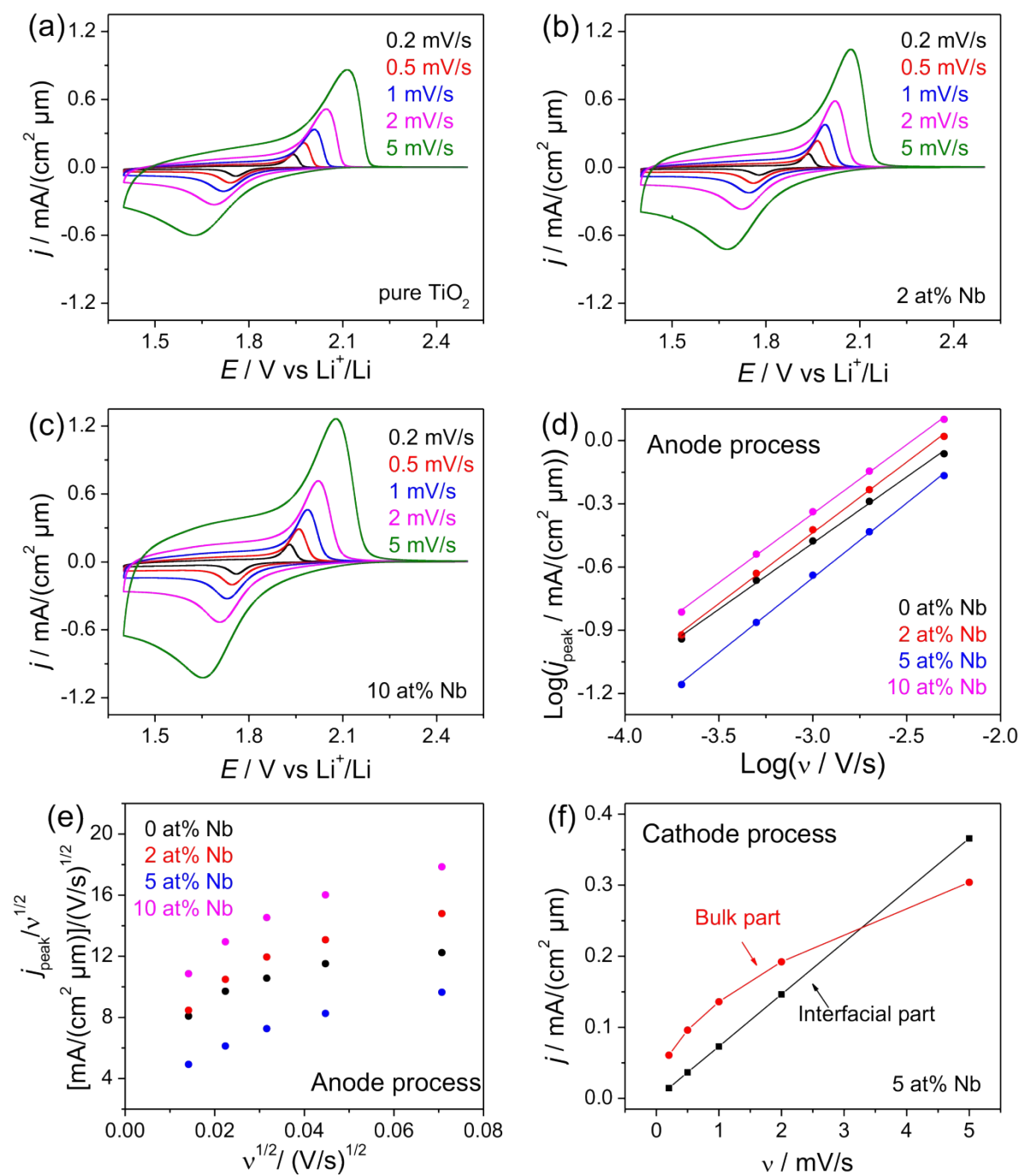
Figure S6. Cyclic Voltammetry data of mesoporous Nb-doped TiO$_2$ films with different doping level in 1 M LiClO$_4$ in propylene carbonate. (a) pure TiO$_2$, (b) 2 at% Nb and (c) 10 at% Nb. (d) Plot of $\log j_{peak}$ *vs.* $\log \nu$. (e) Plot of $j_{peak}/\nu^{1/2}$ *vs.* $\nu^{1/2}$. (f) Currents from the bulk and interfacial part at different scanning rates.

Table S4. Effect of doping level (or rather conductivity) on parameter b (Eq. 3), k_F (Eq. 5), pseudocapacitive contribution, chemical diffusion coefficient of Li (anode process) obtained by using a scanning rate of 1 mV/s.

	σ / S cm^{-1}	b value	k_F value	Pseudocapacity	D_{Li} / cm^2 s^{-1}
TiO$_2$	1×10^{-5}	0.63	7.94	21%	6.3×10^{-16}
2 at% Nb	7.8×10^{-5}	0.67	7.91	30%	6.2×10^{-16}
5 at% Nb	9.8×10^{-5}	0.71	4.28	40%	1.8×10^{-16}
10 at% Nb	7.9×10^{-5}	0.65	10.13	27%	1.0×10^{-15}

Table S5. Overview of used mesoporous films for electrochemical measurements. Surface area was obtained by N$_2$ physisorption as shown in Fig. 7.

	Film area /cm^2	Thickness / μm	Surface area / cm^2
TiO$_2$	4.0	0.36	419
2 at% Nb	3.5	0.16	163
5 at% Nb	4.0	0.16	186
10 at% Nb	4.0	0.15	175
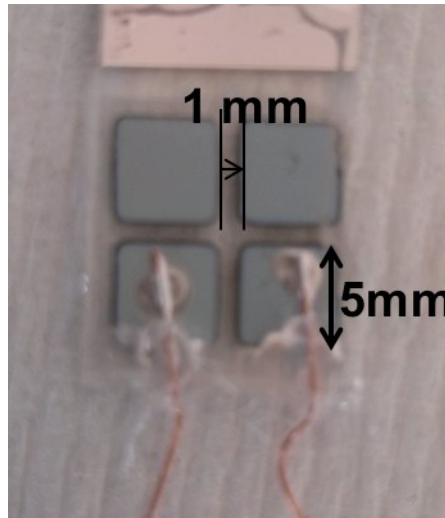
Figure S7. Photograph of conductivity measurement setup.